

1 **Impact of vehicular emissions on the formation of fine particles in the Sao Paulo**
2 **Metropolitan Area: A numerical study with the WRF-Chem model**

3

4 **Angel Vara-Vela¹, M. F. Andrade¹, Prashant Kumar^{2,3}, R. Y. Ynoue¹, and A. G.**
5 **Muñoz^{4,5}**

6

7 ¹Department of Atmospheric Sciences, Institute of Astronomy, Geophysics and
8 Atmospheric Sciences, University of Sao Paulo, Sao Paulo, Brazil

9 ²Department of Civil and Environmental Engineering, Faculty of Engineering and
10 Physical Sciences (FEPS), University of Surrey, Guildford GU2 7XH, United Kingdom

11 ³Environmental Flow (EnFlo) Research Centre, Faculty of Engineering and Physical
12 Sciences, University of Surrey, Guildford GU2 7XH, United Kingdom

13 ⁴International Research Institute for Climate and Society (IRI), The Earth Institute,
14 Columbia University, NY, USA

15 ⁵Centro de Modelado Científico (CMC), Universidad del Zulia, Maracaibo, Venezuela

16

17 Corresponding author: A. V. Vela (angel.vela@iag.usp.br)

18

19 **Abstract**

20 The objective of this work is to evaluate the impact of vehicular emissions on the
21 formation of fine particles (PM_{2.5}; ≤ 2.5 μ m in diameter) in the Sao Paulo Metropolitan
22 Area (SPMA) in Brazil, where ethanol is used intensively as a fuel in road vehicles. The
23 Weather Research and Forecasting with Chemistry (WRF-Chem) model, which
24 simulates feedbacks between meteorological variables and chemical species, is used as
25 photochemical modelling tool to describe the physico-chemical processes leading to

1

evolution of number and mass size distribution of particles through gas-to-particle conversion. A vehicular emission model based on statistical information of vehicular activity is applied to simulate vehicular emissions over the studied area. The simulation has been performed on a 1 month period (7 August - 6 September 2012) to cover the availability of experimental data from the NUANCE-SPS (Narrowing the Uncertainties on Aerosol and Climate Changes in Sao Paulo State) project that aims to characterize emissions of atmospheric aerosols in the SPMA. The availability of experimental measurements of atmospheric aerosols and the application of the WRF-Chem model made it possible to represent some of the most important properties of fine particles in the SPMA such as the mass size distribution and chemical composition in addition to evaluate its formation potential through the gas-to-particle conversion processes. Results show that the emission of primary gases, mostly from vehicles, led to a production of secondary particles between 20-30% in relation to the total mass concentration of $PM_{2.5}$ in the downtown SPMA. $PM_{2.5}$ and primary natural aerosol (dust and sea salt) each contributed with 40-50% of the total PM_{10} (PM_{10} ; $\leq 10 \mu m$ in diameter) concentration. Over 40% of the formation of fine particles, by mass, was due to the emission of hydrocarbons, mainly aromatics. Furthermore, an increase in the number of small particles impaired the ultraviolet radiation and induced a decrease in ozone formation. The ground level O_3 concentration decreased by about 2% when the aerosol-radiation feedback is taken into account.

1. Introduction

The Sao Paulo Metropolitan Area, in the southeast region of Brazil, is considered a megalopolis comprised of Sao Paulo city and more 38 municipalities. One main concern is the occurrence of violations of air quality standards for ozone and fine

particles at different air quality stations from the Sao Paulo Environmental Agency (CETESB). The air pollutant emissions in the SPMA are related to the burning of the fuels: ethanol, gasohol (gasoline with 25% ethanol) and diesel. Recent work of Carvalho et al. (2014) reported a substantial increase in number of vehicles from 1 million in 2000 to almost 7 million in 2014, together with an overview of the pollutants concentration, fuel use in the SPMA and the relationship between the emissions and the improvement in the air quality in past years.

They constitute the main cause of impairment to air quality in SPMA, but the number of air quality standard violations has decreased for almost all pollutants with the exception of $PM_{2.5}$ and O_3 , that, similar to other big cities, impacted by the vehicular emissions, have experienced an increase in the number of violations of their air quality standards as discussed in depth by Carvalho et al. (2014). Perez-Martinez et al. (2014) have analyzed the monthly mean values for the regulated pollutants from 2000 to 2013 for the air quality stations in SPMA and have found that there was a decrease in the average concentration of NO_x , CO, and PM_{10} by 0.65, 0.37, and 0.71 % month⁻¹, respectively, although the sales of the fuels gasoline, ethanol, and diesel had increased by 0.26, 1.96, and 0.38 % month⁻¹ respectively.

A recent report from CETESB (CETESB, 2013) highlighted that, in 2012, the vehicles contributed with about 40% of the total PM_{10} ($\leq 10 \mu m$ in diameter) mass concentrations through direct emissions. If we consider the secondary aerosols, which were about 25% of PM_{10} as estimated by CETESB (2013), these were mainly found to be formed by chemical reactions between gases released from exhaust of vehicles.

The implementation of the Program for the Control of Vehicular Emission (PROCONVE) established by the Brazilian Government in the 80's, enforcing measures such as use of catalytic converters and ethanol as additive to gasoline in substitution of

tetraethyllead, led to decrease in emissions of CO and VOCs and hence their ambient concentration. Although the emissions have been controlled by regulations, in counterpart the number of vehicles has increased substantially and faster than the replacement of the old vehicles by the new ones (Perez-Martinez et al., 2014).

According to CETESB (2013), the road vehicles contributed up to about 97, 87 and 80% of CO, VOCs and NO_x emissions in 2012, respectively. Many studies regarding the air quality impact of the bio-fuels have been performed, especially in Brazil. Anderson (2009) in a review concerning ethanol fuel use in Brazil highlighted that the atmospheric concentrations of acetaldehyde and ethanol are much higher in Brazil comparing to those in other areas of the world. Costa and Sodre (2010) showed that exhaust emissions of hydrous ethanol presented reduced CO and Hydrocarbons (HC), but increased CO₂ and NO_x levels.

A number of past studies has shown the significant participation of the carbonaceous compounds in the concentration of fine particles in the Sao Paulo Metropolitan Area (SPMA) in Brazil (Albuquerque et al., 2011; Miranda and Andrade, 2005; Ynoue and Andrade, 2004; Castanho and Artaxo, 2001). Studies conducted on ambient air pollution in the SPMA have also shown that black carbon (BC) explains 21% mass concentrations of fine particles (PM_{2.5}; ≤2.5 μm in diameter) compared with 40% of organic carbon (OC), 20% of sulfates, and 12% of soil dust (Andrade et al., 2012). Most of the observed ambient PM_{2.5} mass concentration usually originates from precursors gases such as sulphur dioxide (SO₂), ammonia (NH₃), nitrogen oxides (NO_x) and volatile organic compounds (VOCs) as well as through the physico-chemical processes such as the oxidation of low volatile hydrocarbons noted above transferring to the condensed phase (McMurry et al., 2004; Heal et al., 2012). Since these processes are often photo-chemically driven, the resultant aerosol usually falls into the category of

secondary photochemical pollutant (Jenkin and Clemitshaw, 2000). Oxidation of VOCs can produce species of sufficiently low vapor pressure to be condensable, leading to the formation of secondary organic aerosol (SOA) (Kroll and Seinfeld, 2008). Fine particles in SPMA have a great participation on its composition of SOA, formed from the emissions of VOCs, that have the same origin of the primary compounds involved in the formation of ozone, the burning of fuels. The participation of the biogenic emission is considered to be small in the formation of particles in the metropolitan area of the city according to previous studies of Martins et al. (2006).

The impact of the fine particles has been discussed in previous works, with evaluation of the scattering and absorbing effects of the aerosol (e.g. Li et al., 2005; Real et al., 2011). Vehicular emissions of particulate matter (PM) in the SPMA have a high percentage of BC (Brito et al., 2013), which after emitted to the atmosphere can enhance the absorption coefficient and thus the attenuation rates.

One of the most important aspects of this work is the quantitative analysis of the formation of $PM_{2.5}$ and ozone (O_3) in SPMA. Photolysis of O_3 by ultraviolet light in the presence of water vapor is the main source of hydroxyl radical (OH), the most important radical in the atmosphere in terms of reactivity (Monks, 2004). At the same time, OH levels in the atmosphere directly determine the oxidation rate of the precursors of secondary aerosols. Oxidation products of VOCs and semi-VOCs by OH are the most important precursors of SOA (Li et al., 2011a). Although VOCs and NO_x are precursors of both O_3 and a fraction of atmospheric PM (NO_3^- and secondary organics) while they influence indirectly the formation of the rest of the secondary PM components like SO_4^{2-} , their control strategies that are optimal for O_3 controls may even increase $PM_{2.5}$ concentrations (McMurry et al., 2004). Such an analysis is important to evaluate the contribution of the vehicular fleet using different kind of fuels to the

concentration of fine particles. In this sense, a numerical study with an adequate physical approach, representing particles in the modelling system, is important to understand the formation of secondary aerosols from primary emission of gases in a metropolitan area where the composition of fuel in vehicular fleet has changed significantly over the past years. Therefore, the goal of the present study is to evaluate the contribution of vehicular emissions on the formation of fine particles in the SPMA, focusing especially on the potential formation of secondary particles from the primary emission of gases coming from on-road vehicles. The impact of aerosol particles on the ozone photochemistry is also examined by means of numerical simulations. Measurements were performed to provide input data to evaluate the modelling performance and to evaluate the vehicular emission factor. Aerosol measurements were taken from field campaigns that were carried out as part of the NUANCE-SPS (Narrowing the Uncertainties on Aerosol and Climate Changes in Sao Paulo State) project (<http://nuance-lapat.iag.usp.br/>). These campaigns took place between July and September 2012. An online-coupled meteorology and chemistry model, i.e., the Weather Research and Forecasting with Chemistry (WRF-Chem) model, has been used to characterize and describe the physico-chemical processes involved in both the formation and growth of new particles over the SPMA in southern Brazil. The details of the experimental campaigns, WRF-Chem model and emissions are described in Section 2. Results from modelling experiments and comparison with measurements are presented in Section 3. Finally, the summary and conclusions are given in Section 4.

2. Methodology

2.1. Observational datasets

The study period starting from 7 August until 6 September 2012 was selected for comparison with the modelled results (Section 2.2) due to the availability of experimental data from the NUANCE-SPS project. The aim of NUANCE-SPS was to evaluate the impact of emissions in the SPMA on the air quality and changing climatic conditions, and feedback mechanisms between climatic perturbations produced by both primary and secondary emissions and urban atmospheric processes. **Aerosol observation datasets used in this work were collected using a dichotomous sampler (Wedding et al., 1980) and a Micro-Orifice Uniform Deposit Impactor (MOUDI, model 100; MSP Corporation - Marple et al., 1986).** The MOUDI impactor collected particles in 10 size classes with nominal 50% cut-off diameters: 10, 5.6, 3.2, 1.8, 1.0, 0.56, 0.32, 0.18, 0.1 and 0.06 μm . Particles smaller than 0.06 μm were collected in a subsequent stage or after-filter. **The samples collected with the MOUDI impactor were deposited on a polycarbonate membrane filter with 0.4 μm porous and for the Dichotomous sampler the substrate was a teflon membrane filter with 2 μm porous. The after-filter in the MOUDI impactor is a 33 mm teflon membrane filter, that was not submitted to the reflectance analysis.** The collected membrane filters sampled with the Dichotomous and MOUDI samplers were analyzed to the identification of trace elements of mass through X-ray diffraction analysis, mass concentration through gravimetric analysis, and black and organic carbon through reflectance and thermo analysis using a thermal-optical transmittance (TOT) (Sunset Laboratory Inc. – Birch and Cary, 1996). Ion concentrations were evaluated through the ion chromatography analysis of the soluble material collected on the membrane filters (sulphate, nitrate, ammonium, sodium, and chloride). **All these samplings were performed on the roof of the main building of the Institute of Astronomy, Geophysics and Atmospheric Sciences of the University of Sao Paulo (IAG-USP) (hereafter also referred as IAG-USP)**

measurement site or simply IAG-USP), which is inside a small green-park (approximately 7.4 km²), with local traffic during the day and surrounded by major roads with intense traffic by light and heavy-duty vehicles (Nogueira et al., 2014). Table 1 lists the aerosol instrumentation deployed roughly at the IAG-USP measurement site. In addition, ambient data from the CETESB's air quality monitoring network and the IAG-USP's climatological station (hereafter also referred as AF-IAG) were also considered for evaluation of numerical simulations. The locations of measurement sites are depicted in Fig. 1 whereas geographic coordinates and the list of pollutants and meteorological parameters monitored at each site is available in Table 2.

2.2. WRF-Chem model

The WRF-Chem model is a fully coupled online meteorological and chemical transport model (Grell et al., 2005), supported by National Center for Atmospheric Research (NCAR) of the USA and several other research institutions around the world. This model is a system of two key components. The WRF-Chem meteorological component, the Weather Research and Forecasting (WRF), is a system configured for both research and operational applications. The dynamical core used in this study is the Advanced Research WRF (ARW). Model's equations into ARW are solved to non-hydrostatic conditions on a fully compressible atmosphere. Further details on the modelling system can be found on the WRF model website (<http://www.wrf-model.org>). On the other hand, the WRF-Chem chemical component treats chemical processes such as dry deposition, gas-phase chemistry, photolysis rates, and aerosols chemistry. A detailed description of the WRF-Chem model can be found on its website (<http://ruc.noaa.gov/wrf/WG11>). Since both meteorological and chemical components are fully coupled, the transport of all chemical species is on-line. The gas-phase

chemistry and aerosol modules employed in this study are the Regional Acid Deposition Model, version 2 (RADM2) (Chang et al., 1989) and the Modal Aerosol Dynamics Model for Europe - Secondary Organic Aerosol Model (MADE - SORGAM) (Ackermann et al., 1998; Schell et al., 2001), respectively. The inorganic species included in the RADM2 mechanism are 14 stable species, 4 reactive intermediates, and 3 abundant stable species (oxygen, nitrogen and water). Atmospheric organic chemistry is represented by 26 stable species and 16 peroxy radicals. The RADM2 mechanism represents organic chemistry through a reactivity aggregated molecular approach (Middleton et al., 1990). Similar organic compounds are grouped together in a limited number of model groups through the use of reactivity weighting. The aggregation factors for the most emitted VOCs are given in Middleton et al. (1990).

On the other hand, the most important process for the formation of secondary aerosol particles is the homogeneous nucleation in the sulfuric acid-water system. It is parameterized in MADE, following the method of Kulmala et al. (1998). Aerosol growth by condensation occurs in two steps: the production of condensable material (vapor) by the reaction of chemical precursors, and the condensation and evaporation of ambient volatile species on aerosols. The inorganic chemistry system, based on the Model for an Aerosol Reacting System (MARS) (Saxena et al., 1986) and its modifications by Binkowski and Shankar (1995), calculates the chemical composition of a sulphate-nitrate-ammonium-water aerosol according to equilibrium thermodynamics. The organic aerosol chemistry is based on the SORGAM, which assumes that SOA compounds interact and form a quasi-ideal solution (Grell et al., 2005). The SOA formation in SORGAM follows the two-product approach (Odum et al., 1996) where the oxidation of hydrocarbons produces two types of modelled semivolatile compounds that are partitioned between the gas and particle phases after

considering the absorptive partitioning theory (Pankow, 1994a, b). The primary organic aerosol (POA) in MADE is calculated from the primary anthropogenic emission of OC. Then, one may calculate the predicted OC concentration from the sum of both SOA and POA. The concurrent organic matter (OM) can be obtained from the OC concentration by application of a conversion factor. Brown et al. (2013) showed that the average OM:OC ratio was 1.54 (with a standard deviation of 0.2) for sites with low amount of secondary aerosol formation. It is important to note that this ratio can change from one place to another. In areas impacted by biomass burning the ratio can be higher. Gorin et al. (2006) assumed a ratio of 1.6 for the conversion from OC to OM over an area that experiences a significant wood smoke influence.

2.2.1. Model configuration

WRF-Chem version 3.5 was configured with three nested grid cells: coarse (75 km), intermediate (15 km) and fine (3 km). The coarse grid cell covered a big region of Brazil and also of the Atlantic Ocean. The intermediate grid covered the southeast Brazil while the fine grid cell covered barely the SPMA and metropolitan areas nearest to it. Fig. 1 shows the arrangement of measurement sites and topography in the downtown area of the 3-km modelling domain. The initial and boundary meteorological conditions are from the National Center for Environmental Prediction's Final Operational Global Analysis with 1° of grid spacing, 26 vertical levels and are available every six hours: 00, 06, 12 and 18 UTC (<http://rda.ucar.edu/datasets/ds083.2/>). The initial and boundary chemical conditions for representing gases and aerosols background concentration were obtained from the Model for Ozone and Related chemical Tracers, version 4 (MOZART-4; Emmons et al., 2010). This model was driven by meteorological inputs from the Goddard Earth Observing System Model, version 5 at

a horizontal resolution of $1.9^{\circ} \times 2.5^{\circ}$, 56 vertical levels that are also available every six hours. Table 3 lists the WRF-Chem configuration options employed by this study.

WRF-Chem simulation with coupled primary aerosol (dust, sea salt and anthropogenic) and gas (biogenic and anthropogenic) emission modules, together with the direct effect of aerosol particles turned on, is performed as the control simulation in order to evaluate the model performance (hereafter referred to as Case_0). For secondary aerosols, a simulation scenario (Case_1) with biogenic and anthropogenic gases emission is performed to evaluate its formation potential. An additional simulation (Case_2) is also performed to evaluate the impact of aerosols on ozone photochemistry. Notation and description of simulations are listed in Table 4. The first seven days of each simulation were not analyzed and used for model spin-up.

2.3. Emissions

2.3.1. Anthropogenic emissions

Anthropogenic emissions of trace gases and particles in both 3 and 15-km modelling domains were considered to include emissions only coming from on-road vehicles through the use of a vehicular emission model developed by the IAG-USP's Laboratory of Atmospheric Processes (LAPAt). Basically, this model considers the number of vehicles, vehicular emission factors, and average driving kilometers for vehicle per day as basic parameters for the calculation of exhaust emissions considering different vehicle types (light-duty vehicles, heavy-duty vehicles, and motorcycles) and different fuel types (ethanol, gasohol, combination of any proportion of gasohol and ethanol, and diesel) according to CETESB (2012). The details of this model are available in Andrade et al. (2015). In the case of VOCs, there are other two relevant emissions (fuel transfer and evaporative processes) associated with the vehicles, besides

the exhaust emissions. Because of the complexities in the spatial representation due to a numerous factors such as emissions at service stations, such emission sources are assumed to be emitted by exhaust of vehicles for the sake of simplicity. The vehicular fleet and intensity of use datasets are provided by the National Department of Traffic (DENATRAN) and the Sao Paulo Transporte (SPTrans), respectively. Emission factors for road vehicles for most pollutants were considered from previous studies performed inside the road tunnels (i.e. Janio Quadros, referred as JQ tunnel, and the tunnel 3 of the Rodoanel Mario Covas that is referred hereafter as RA tunnel) located within the SPMA (Pérez-Martínez et al., 2014; Nogueira et al., 2014). However, emission factors for VOCs are considered from dynamometer protocols (CETESB, 2010). VOCs and particulate matter speciation profiles used by pas-phase and aerosol chemical modules were also obtained from NUANCE-SPS experimental campaigns performed in 2011 (tunnel measurements) and 2012 (ambient data). It is important to note that due to the lack of information on vehicular emission factors and intensity of use for most of the other metropolitan areas inside both modelling domains (e.g. the Campinas Metropolitan Area, the second largest grey stain in Fig. 2), the calculation of vehicular emissions for these urban areas was carried out on the basis of the parameters found for the SPMA. The number of vehicles in any modelling domain is calculated from the sum of the number of vehicles in each one of the main urban areas inside the modelling domain in question.

Spatial distribution of emissions for the 3-km modelling domain resolution was based on road density products compiled by the OpenStreetMap project and extracted from the Geofabrik's free download server (<http://download.geofabrik.de>). Urban areas were assumed to allocate high emissions since these concentrate a road density greater than other areas. In the case of the 15-km modelling domain, emissions are based on

night-time lights data from the Defense Meteorological Satellite Program (<http://ngdc.noaa.gov/eog/dmsp/downloadV4composites.html>). These images are 30 arc second grids, spanning -180° to 180° longitude and -65° to 75° latitude and contain the lights from cities, towns and other sites with persistent lighting, including gas flares. Cleaned up night-time light points with no ephemeral events such as fires are used to allocate emissions. To estimate the number of vehicles in each grid point of both domains, the sum of individual intensities at each point (i.e. total road length for the 3-km modelling domain and night-time light for the 15-km modelling domain) is firstly normalized by the total fleet, and then distributed uniformly using the total fleet distribution so that emissions in urban areas are mainly represented by emissions coming from their vehicles. Furthermore, due to the complexity involved in describing the temporal variation of emissions at each grid point, median values for vehicular traffic obtained from measurements inside the JQ and RA tunnels (Pérez-Martínez et al., 2014) were used for distributing the emissions during the day in both domains. This approximation followed the approach used by Fast et al. (2006) where emission profiles were calculated from median diurnal variations on weekdays and weekends. We have applied the same constant diurnal cycle at all grid points where emissions have values greater than zero. VOC and PM emission profiles were assumed to be the same as for CO and NO_x emission profiles since these pollutants are also characteristic tracers of emissions of light-duty and heavy-duty vehicles, respectively. Fig. 2 shows the maximum hourly emission rates for aromatic VOCs in the 3-km modelling domain. Anthropogenic emissions were not considered in the 75 km modelling domain.

The Another Assimilation System for WRF-Chem (AAS4WRF) chemical emissions pre-processor developed by the Latin American Observatory (OLE2; Muñoz et al., 2010; 2012) was used to scale emission rates on WRF curvilinear coordinates.

AAS4WRF is appropriate to write chemical emission rates from both surface and elevated sources in the proper WRF data file format, providing an alternative tailored way to assimilate emissions to WRF-Chem. The method is explained in the OLE2 Wiki pages in detail (http://www.cmc.org.ve/mediawiki/index.php?title=Calidad_de_Aire).

2.3.2. Other emissions

Biogenic emissions are calculated online based on the Guenther scheme (Guenther et al., 1993; 1994). The Guenther biogenic emissions model calculates the emission rates using temperature, photo-synthetically active radiation flux and land-use data as the U.S. Geological Survey (USGS) land-use cover system classification if coupled with the WRF model. However, as indicated in the WRF-Chem emissions guide (http://ruc.noaa.gov/wrf/WG11/Emission_guide.pdf), several key chemical species would have been representing relatively low emission rates because of the limited vegetation types in the simulation, and thus their impacts are anticipated to be much lower than those from vehicular emissions.

Dust and sea salt emissions are calculated online following the works of Ginoux et al. (2001) and Gong (2003), respectively. The calculation of Ginoux et al. (2001) for the uplifting of dust particles is based on the surface wind speed, wetness and information on soil characteristics. The model then solves the continuity equation including the emission, chemistry, advection, convection, diffusion, dry deposition, and wet deposition of each species. The parameterization of sea salt aerosol source function of Gong (2003) is an extended parameterization of Monahan et al. (1986) which scales the generation of marine aerosols from mechanical disruption of wave crests by the wind and sea surface covered by whitecaps.

3. Results and discussion

3.1. Characterization of meteorological conditions

In order to study and understand the spatial and temporal variability of atmospheric aerosols, O₃, and other pollutants during the study period, it was first necessary to analyze the behavior of main meteorological systems acting on the atmospheric environment of the SPMA and surrounding areas.

According to the monthly climate reports from the IAG-USP's Climate Research Group (GrEC), the observed precipitation rates were lower than the climatological value in SPMA (-38.6 mm) and larger part of the Sao Paulo State during August 2012. Negative anomalies on the precipitation were caused by the intensification of the South Atlantic Subtropical High (SASH). These conditions established an easterly wind anomaly pattern at the 850 hPa level. Conditions were unfavorable for relative humidity coming from the Amazon due to the Low Level Jet (LLJ) and less intense Alisian winds in the Tropical Atlantic (GrEC, 2012a). However, the action of frontal systems favored the rain accumulation in September 2012, mainly in western Sao Paulo State where the greater positive amount of anomalies was observed. Precipitation events were predominantly observed during the second half of the month. In this case, the wind pattern showed an opposite configuration to that observed in August 2012 as a result of the weakening of the SASH (GrEC, 2012b). The IAG-USP's climatological station recorded an accumulated precipitation of about 1.3 mm on three days of occurrence (28 August, 30 August and 4 September 2012) and an easterly wind pattern with a median intensity of 2 m s⁻¹ during the period between 07 August and 06 September 2012. Fig. 3 shows the hourly accumulated precipitation and relative humidity observed at the IAG-USP's climatological station.

3.2. Analysis of aerosol species

Aerosol analysis included species such as organic carbon (OC), elemental carbon (EC), sulphate, nitrate, ammonium, sodium and chloride in addition to other elemental constituent of PM. All the sampling for these species were performed at IAG-USP. Results showed that the major contributors to the concentration of fine particles are OM (55.7%; OM:OC ratio of 1.5 found by Brito et al. (2013)) and EC (15%), followed by sulphate (2.9%), ammonium (2.1%), sodium (1.9%), nitrate (0.5%) and chloride (0.3%). The remaining mass (21.6%) is calculated by determining of the difference between the total mass of PM_{2.5} (from the gravimetric analysis) and the sum of the masses of 7 individual compounds, as noted above. Part of this remaining mass is related to the water content of aerosols (Andrade et al., 2012).

On the other hand, PM_{2.5}, PM₁₀ and size distribution of particles measured at IAG-USP show that the study period was characterized by a reduction in the concentrations up to the end of August 2012 when their minimum values were achieved. This reduction was related to the action of a semi-stationary front between the coasts of Sao Paulo and Parana States. After the passage of this system, aerosol concentrations have significantly increased what could be related to an increase in relative humidity once the SASH system is moved away from the continent, as well as the transport of aerosol particles produced by forest fires in the central-west region of Brazil and the Sao Paulo State. Several studies have shown the contribution of forest fires on the atmospheric aerosol concentrations in SPMA (Vieira-Filho et al., 2013; ~~Lopes et al., 2012~~; Vasconcellos et al., 2010). One way to qualitatively evaluate the contribution of forest fires on aerosol concentrations is by using the air mass trajectories. The Hybrid Single-Particle Lagrangian Integrated Trajectory (HYSPLIT) model (Draxler and Hess,

1998) was used to calculate backward trajectories of air masses in order to identify atmospheric transport of air mass from forest fire areas. Fig. 4 shows the three-day backward trajectories of air masses starting at IAG-USP for the days 9 and 31 August and 5 September, when increases in the OC and EC concentrations were observed at IAG-USP. The pink markers on the map represent the observed fire locations during the study period considering different satellite products (GOES, AQUA, TERRA, NOAA).

Fig. 5 shows the concentration of OC, EC and some species of $PM_{2.5}$ during the study period at IAG-USP. We can observe eleven exceedances of $PM_{2.5}$ concentration with respect to the air quality standard of $25 \mu g m^{-3}$ (see grey line in Fig. 5a) established by the World Health Organization (WHO). These exceedances have mainly occurred at the beginning and at the end of the study period when an increase in the concentrations of OC and EC were observed. The increasing organic matter could be associated to traffic incidents which may raise the emissions, that, in case of less favorable meteorological conditions (e.g. lower height of lower planetary boundary layer, PBL, or slow transport of air pollutants) may have led to a more efficient formation of secondary particles. Castanho and Artaxo (2001) analyzed the behavior of the aerosol composition in SPMA and showed the increase in the concentration of inorganic and organic material in the winter season compared to the summer season, explaining this behavior with the meteorological characteristics: dry conditions with low height inversion layer in the wintertime and a rainy summer.

Size distributions of aerosol mass indicate that the majority of sulphate, ammonium and PM_{10} mass concentration is distributed in the size range with diameters between 0.1 and $1 \mu m$, commonly known as accumulation mode particles (Kumar et al.,

2010). In the cases of nitrate, sodium, and chloride, most part of mass was concentrated in particles with diameters greater than 1 μm .

3.3. Comparison of baseline simulation with observations

All the numerical results presented in this section, for the purpose of comparison with the measurements, were obtained from the baseline simulation (Case_0). The predicted temperature, humidity, and wind distribution have been compared to measurements from the AF-IAG and INT measurement sites. Overall, the model captured the diurnal variation of temperature, humidity, and wind directions reasonably well. However, the predicted wind speeds were slightly lower than the observed values. To evaluate the model performance in solving the meteorology and chemical species, we computed the statistics correlation coefficient (R), Bias (B), and root mean square error UB (RMSE_{UB}). The definitions of these statistics are given in the Appendix. Table 5 presents the summary of these statistics, showing comparisons between WRF-Chem predictions and observations. Fig. 6 shows the predicted average of wind vectors at 10m and temperature at 2m for the whole study period in the 3-km modelling domain. Blue dots represent the locations of AF-IAG and INT sites, while the numbers in cyan indicate the observed average temperatures (i.e. 17.7 °C at AF-IAG and 17.8 °C at INT). On an average, the predicted wind direction was easterly in SPMA, which has somewhat affected the spatial distribution of aerosol particles as examined later in this section. Likewise, a good agreement is found between the predicted PM_{2.5}, PM₁₀ and O₃ concentration and measurements at most of the sites. Figs. 7, 8 and 9 show the observed and predicted temporal variations of PM_{2.5}, PM₁₀ and O₃ concentrations at 3, 10 and 6 sites in the SPMA, respectively, with some measurement sites sharing the same grid point for comparisons due to the geographical proximity. These figures suggest that

predicted concentrations did not present any significant spatial variation in the downtown SPMA and were generally underestimated when compared to measurements. This under prediction could be associated with an underestimation on the vehicular emissions as well as other emission sources (e.g. emissions coming from industry) that are disregarded in this study. **The high concentrations of $PM_{2.5}$ and PM_{10} observed at the beginning and at the end of the study period, whose variability and trends were reasonably well captured by the model, could be related with the emission of high aerosol loadings due to traffic incidents as well as the establishment of lower PBL heights, commonly observed under post-frontal situations.** The results for this simulation (Case_0) show that overall the predicted PBL heights (not shown here) have a regular diurnal variation in the downtown SPMA with averaged daily values around 500 m at both the beginning and the end, and of up to 700 m in the middle of the study period, when lower concentrations of aerosols were observed. Statistics to quantify the model performance in the representation of $PM_{2.5}$, PM_{10} and O_3 concentrations can be visualized along with the Taylor Diagram (Taylor, 2001) shown in Fig. 10. **In general, most of evaluated parameters present good correlation coefficients, mainly those for PM_{10} , but with negative biases and standard deviations lower than those for observations.** The mean biases for $PM_{2.5}$, PM_{10} and O_3 concentrations were $-8.84 \mu g m^{-3}$, $-14.13 \mu g m^{-3}$ and $-0.85 ppb$, respectively (see Table 5).

Figures 11 - 13 show the predicted average surface distribution of $PM_{2.5}$, PM_{10} and $PM_{2.5}:PM_{10}$ ratio for the 3-km modelling domain, respectively. Red dots and cyan numbers represent the locations and the observed mean PM concentrations (or mean PM concentration ratios) at the measurement sites, respectively. Major contributions of $PM_{2.5}$ on the total PM_{10} concentration were observed mainly over offshore continental areas (see Fig. 13). High $PM_{2.5}:PM_{10}$ concentration ratios would be firstly associated

with the transportation of fine particles and gases from upwind regions (see Fig. 6), followed by a production of fine particles from biogenic emissions. Additional comparisons between the observed and predicted concentrations of OC and EC at IAG-USP (the only site with measurements of OC and EC) are shown in Fig. 14. In addition to an underestimation of emissions, under predicted OC concentrations could also be associated with an underestimation of SOA probably due to the absence of oxidation of monoterpenes and a limited treatment of anthropogenic VOCs oxidation in the RADM2 mechanism, as discussed by Tuccella et al. (2012). The SORGAM aerosol module considers the formation of anthropogenic SOAs from the oxidation of alkane, alkene and aromatic VOCs as well as the biogenic SOA formation from the oxidation of alpha-pinene, limonene and isoprene VOCs. Recent studies coupling non-traditional SOA models (volatility basis set approaches) in WRF-Chem show improvements in the predicted SOA concentrations, although these are still lower than those observed (e.g. Li et al., 2011b; Ahmadov et al., 2012; Shrivastava et al., 2013).

On the other hand, measurements of mass size distribution were also made with a MOUDI impactor at IAG-USP, following the protocol describe in Miranda and Andrade (2005). Constituents of aerosol were subsequently determined by X-Ray fluorescence analysis and ion chromatography analysis. As previously indicated in this section, the main identified species are SO_4 , NO_3 , NH_4 , Na and Cl. The observed average aerosol composition is derived using measurements from both MOUDI impactor and SUNSET analyzer. To perform the comparisons of mass size distribution, we adequately joined the MOUDI bin sizes according to the three modes used by the MADE aerosol module: Aitken ($<0.1 \mu\text{m}$), accumulation ($0.1\text{-}1 \mu\text{m}$) and coarse ($>1 \mu\text{m}$). The observed and predicted aerosol mass size distributions averaged over the same sampling time period (16 days along the study period) are shown in Fig. 15. Over the

downtown SPMA, both the observed and predicted fine particles from accumulation mode account for majority of the total $PM_{2.5}$ mass. Since the formation-growth processes of aerosols in question are explicitly treated in the Aitken and accumulation modes, the predicted concentrations for particles larger than $1\ \mu m$ are assumed to be zero. In this case, the mass of particles larger than $1\ \mu m$ is allocated to the PM_{10} aerosol variable (see Fig. 15). The comparison between the observed and predicted average contributions for the main identified aerosol constituents at IAG-USP is shown in Fig. 16. Both the observed and predicted OC and EC make up the largest fraction of $PM_{2.5}$ mass with contributions of 55 and 40%, respectively. In addition, it was found that the predicted SOA concentrations contribute 17% of the predicted total OC concentration at this measurement site. Various global and regional scale SOA simulations have been conducted using mass-based yield and partitioning coefficients, but they have underestimated the SOA concentrations by roughly an order of magnitude, especially over urban regions (Matsui et al., 2014). Using the same SOA formation approach employed by this study and a conversion factor of 1.6 to convert the emissions of OC to OM, Tuccella et al. (2012) found simulated SOA:OM ratios in the range between 5-40% against 50-80% observed. Although the predicted average $PM_{2.5}$ concentration ($14.48\ \mu g\ m^{-3}$) was lower than observed ($22.32\ \mu g\ m^{-3}$), the mean aerosol chemical composition was reasonably well represented by the model (see Fig. 16).

3.4. Contribution of dust, sea salt, and coarse anthropogenic aerosols to PM_{10} concentration

The evaluation of the contribution of dust and sea salt aerosols on PM_{10} concentration is performed from the sum of their concentrations divided by the PM_{10} concentration. The simulated average ratio between dust – sea salt aerosols and the total PM_{10} mass concentration is shown in Fig. 17b. High concentration ratios have been

observed over the ocean where sea salt emissions are by far the most important aerosols source. Unlike high concentration ratios over the ocean, lower concentration ratios are observed over the continent far away from the coast. In this region, the main sources of atmospheric aerosols would be the emission of primary biological aerosol, SOA formed from the emission of biogenic volatile organic compounds (BVOCs), and forest fires. However, particles could also be transported from remote areas. In addition, we can also observe that dust and sea salt aerosols have a contribution between 40 and 50% of the total PM_{10} concentration in the downtown SPMA. Furthermore, it is possible to estimate the contribution of all the other PM_{10} (i.e., the coarse anthropogenic aerosol) to the total PM_{10} mass concentration. It may be directly calculated from the model or estimated from the Figs. 13 and 17b once the sum of concentrations of $PM_{2.5}$, dust and sea salt, and coarse anthropogenic aerosol represents 100% of the total PM_{10} mass concentration. For example, we found that the coarse anthropogenic aerosol represents around 10% of PM_{10} in the downtown SPMA.

3.5. Evaluation of secondary aerosol formation

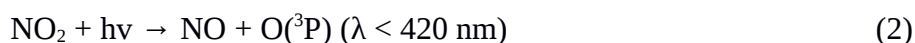
As described in Section 2.1, the aerosol module employed by this study (MADE/SORGAM) includes the homogeneous nucleation in the sulphuric acid-water system. The sulphuric acid is the most significant condensable molecule formed in the atmosphere, which has also been long recognised as the most important molecule from the point of view of the nucleation of new particles (Jenkin and Clemitshaw, 2000; Seinfeld and Pandis, 2006). But, for the SPMA, the importance of SOA formed from the anthropogenic emission of fuel used by the transport sector was noted (Salvo and Geiger, 2014). According to the official emission inventory developed by the Sao Paulo Environmental Protection Agency (CETESB, 2013), the SOA explains 51% of the fine particle mass concentration, with the vehicular emission being its main source. The

subsequent growth processes involve aerosol growth by condensation of condensable material onto existing particles, and by coagulation of particles to form larger particles (Kumar et al., 2011; 2014). For example, particles in the accumulation mode emerge through coagulation of particles from the Aitken mode (Kumar et al., 2011). It is important to emphasize that the boundaries were updated with gas and aerosol background concentrations coming from the 15-km modelling domain during the whole simulation period. Thereafter, the impact of vehicular emissions on the formation of fine particles was calculated from the predicted $PM_{2.5}$ concentration considering an emission scenario (Case_1) in which only emission of gases from vehicles and vegetation are taken into account to be emitted to the atmosphere from the surface. The predicted average $PM_{2.5}$ (Case_1): $PM_{2.5}$ (Case_0) ratio is shown in Fig. 17a. A contribution between 20 and 30% in the predicted baseline $PM_{2.5}$ concentration in downtown SPMA is found to correspond to the fine particles formation and transportation processes. Higher concentration ratios over the SPMA surroundings (30-50%) could be associated with more efficient biogenic emissions. Overall, it is observed that the formation efficiency increases towards the northwest from the ocean. Deep red areas in Fig. 17a could also be associated with the transportation of fine particles and gases from other regions, in addition to having a more efficient production of fine particles from biogenic emissions. For example, given the distribution of winds in Fig. 6, the northern boundary could represent the main source of particles and gases over this part of the simulation domain. Additionally, the comparison between the predicted and observed OC and EC concentrations at IAG-USP shown in Fig. 14 includes the Case_1 simulation in which only emission of primary gases is taken into account in the assessment of fine particles formation. The concentration peaks observed at the beginning and at the end of the study period may be associated with the transport of aerosol particles from both biomass

and fossil fuel burning areas (see Fig. 4). Considering the Case_1 simulation, we can observe very low concentrations for EC (mean concentration of $0.01 \mu\text{g m}^{-3}$), as expected. This is because these particles are not produced by photochemical processes in the atmosphere, but associated mainly with the diesel exhaust.

3.6. Aerosol impact on O_3 photochemistry

Ozone photochemistry production mainly depends on the two key photolysis rates, as shown in Eqs. (1) and (2) below (i.e., shortwave radiation able to reach the surface to break molecules of O_3 and NO_2). Therefore, the impact of aerosols on O_3 photochemistry has been evaluated from the impact of aerosols on downward shortwave radiation. Attenuation (scattering and absorption) of downward shortwave radiation by aerosols may substantially modify the photolysis rates, and thereby affecting the ozone photochemistry production.



The average percentage change in surface O_3 concentrations at 16:00 LT with and without the aerosol-radiation feedback module turned on are shown Fig. 17c. Overall O_3 is destroyed or formed (incoming transport from other regions) in small quantities between -1 and 1% in relation to its total concentration. In addition, it was observed that the surface O_3 concentration decreased by around 2% in the downtown SPMA. Li et al. (2011a) found that the impact of aerosols on O_3 formation in Mexico City was most pronounced in the morning with the O_3 reduction of 5-20%, but the reduction is less than 5% in the afternoon. Low reductions in the O_3 concentration in the downtown SPMA compared to results from other studies may be explained by the lower

predicted PM₁₀ concentrations, which can lead to a minor attenuation of the incoming solar radiation. Simulated mean downward shortwave fluxes at ground surface (not shown) were up to 5% higher for the Case_2 than for the Case_0 during the afternoon. The inclusion of the direct effect of aerosol particles was found to have small reductions in the surface temperature (changes by around 2%), presumably due to an increase in the number of atmospheric processes involving downward longwave fluxes over this area. Forkel et al. (2012) found an underestimation of predicted downward longwave radiation over the southern Baltic Sea when the direct effect of aerosol particles was neglected. Despite the highly non-linear behavior of tropospheric O₃, the reduction in the predicted O₃ concentrations indicates a high efficiency of aerosols to attenuate the downward shortwave radiation, what is plausible once it was found that low PM₁₀ concentrations have a capability to reduce ground level O₃ concentrations in a few ppb.

4. Summary and conclusions

The WRF-Chem community model has been used to evaluate the impact of vehicular emissions on the fine particles formation in the SPMA. Three thirty-one day simulations covering a period from 7 August to 6 September 2012 have been performed. The aims were to evaluate the impact of fine particles formation (both inorganic and SOA) from gases emitted by road vehicles as well as the aerosol impacts on the ozone formation photochemistry. The results were compared with the measurements available from the NUANCE project.

The predicted temporal variations of meteorology, PM_{2.5}, PM₁₀ and O₃ were found to agree well with the measurements at most of the sites during the entire simulation period. However, the predicted concentrations of PM_{2.5}, PM₁₀ and O₃ (but in minor intensity) were lower than the observed values. This difference could be

associated with an underestimation of the vehicular emissions and other emission sources such as industry, heating and cooking, which are not considered in this study. Wind speed and direction played an important role in the distribution of fine particles over the simulation domain. Backward trajectories analysis suggested that aerosol particles from biomass burning were transported to SPMA, impacting on the PM concentration over this region.

The baseline simulation (Case_0) showed that dust and sea salt aerosols made a contribution between 40 and 50% of the total PM_{10} concentration in the downtown SPMA. On the other hand, the Case_1, which represents simulations with gaseous emissions only, indicates that the emissions of primary gases coming mainly from vehicles have a potential to form new particles between 20 and 30% in relation to the baseline $PM_{2.5}$ concentration found in the downtown SPMA. Finally, the Case_2, which represents simulations with aerosol-radiation feedback turned on, reveals a reduction in the surface O_3 concentration by around 2% in the afternoon (16:00 LT) when the aerosol-radiation feedback is taken into account.

This study provides a first step to understand the impact of vehicular emissions on the secondary particles formation in the SPMA. Nevertheless, more experimental campaigns are recommended for future work in order to characterize aerosols in ambient air and to improve their emission estimates so that a better understanding of physical and chemical properties and their formation can be established. This study also evaluates the importance of the VOCs in the formation of not only O_3 but also of fine particles. These compounds play an important role concerning health impacts and climate change, and the control of their concentrations requires the description of their formation mechanisms.

Appendix A

The statistics used in this study are defined as follows.

1. Correlation coefficient (R):

$$R = \frac{\sum_{i=1}^N (M_i - \bar{M})(O_i - \bar{O})}{\sqrt{\sum_{i=1}^N (M_i - \bar{M})^2} \sqrt{\sum_{i=1}^N (O_i - \bar{O})^2}}$$

2. Root mean square error UB (RMSE_{UB}):

$$RMSE_{UB} = \sqrt{\frac{1}{N} \sum_{i=1}^N [(M_i - \bar{M}) - (O_i - \bar{O})]^2}$$

3. Bias (B):

$$B = \frac{1}{N} \sum_{i=1}^N (M_i - O_i)$$

where

$\bar{O} = \frac{1}{N} \sum_{i=1}^N O_i$ and $\bar{M} = \frac{1}{N} \sum_{i=1}^N M_i$ are the average values of the individual observed

and predicted values, O_i and M_i , respectively. N is the number of observations.

5. Acknowledgments

Prashant Kumar, Angel Vara-Vela and Maria de Fatima Andrade thank the University of Surrey's International Relations Office for the Santander Postgraduate Mobility Award that helped Angel Vara to visit University of Surrey, UK, and develop this research article collaboratively. The authors from Universities of Surrey and Sao

Paulo also acknowledge the collaborative funding received through the University Global Partnership Network (UGPN) to the project titled “*Emissions And Role Of Fine Aerosol Particles In Formation Of Clouds and Precipitation (eRAIN) - A demonstration study for the megacity, São Paulo*” for supporting this research work. Maria de Fatima Andrade and Angel Vara-Vela acknowledged funding from the Coordination for the Improvement of Higher Education Personnel (CAPES) and Research Foundation of the State of Sao Paulo (FAPESP, project 2008/58104-8) that allowed the experimental campaigns. The authors also thank the WRF-Chem developers, the NOAA's National Geophysical Data Center, the NCAR's Data Support Section and Atmospheric Chemistry Division, the Latin American Observatory (OLE2), the Sao Paulo Environmental Protection Agency (CETESB), the OpenStreetMap Data Extracts, and the NCAR Command Language (NCL) software for providing the tools and datasets used in this research.

6. References

- Ackermann, I. J., Hass, H., Memmesheimer, M., Ebel, A., Binkowski, F. S., and Shankar, U.: Modal aerosol dynamics model for Europe: development and first applications, *Atmos. Environ.*, 32, 2981-2999, 1998.
- Ahmadv, R., McKeen, S. A., Robinson, A. L., Bahreini, R., Middlebrook, A. M., de Gouw, J. A., Meagher, J., Hsie, E. Y., Edgerton, E., Shaw, S., and Trainer, M.: A volatility basis set model for summertime secondary organic aerosols over the eastern United States in 2006, *Journal of Geophysical Research*, 117, D06301, doi:10.1029/2011JD016831, 2012.

683 Albuquerque, T. T. A., Andrade, M. F., and Ynoue, R. Y.: Characterization of
684 atmospheric aerosols in the city of Sao Paulo, Brazil: comparisons between
685 polluted and unpolluted periods, *Water Air Soil Pollution*, 195, 201-213, 2011.

686 Anderson, L.: Ethanol fuel use in Brazil: air quality impacts, *Energy Environ. Sci.*, 2,
687 1015-1037, 2009.

688 Andrade, M. F., Ynoue, R. Y., Freitas, E. D., Todesco, E., Vara-Vela, A., Ibarra, S.,
689 Martins, L. D., Martins, J. A., Carvalho, V. S. B.: Air quality forecasting system
690 for Southeastern Brazil, *Frontiers in Environmental Science*, 3, 1-14, 2015.

691 Andrade, M. F., Fornaro, A., Miranda, R. M., Kerr, A., Oyama, B., Andre, P. A., and
692 Saldiva, P.: Vehicle emissions and PM_{2.5} mass concentrations in six
693 Brazilian cities, *Air Quality, Atmosphere and Health*, 5, 79-88, 2012.

694 Binkowski, F. S. and Shankar, U.: The regional particulate matter model, 1. Mode
695 description and preliminary results, *Journal of Geophysical Research*, 100,
696 26191-26209, 1995.

697 Birch, M. E., and Cary, R. A.: Elemental carbon-based method for occupational
698 monitoring of particulate diesel exhaust: methodology and exposure issues,
699 *Aerosol Science and Technology*, 25, 221-241, 1996.

700 Brito, J., Rizzo, L. V., Herckes, P., Vasconcellos, P. C., Caumo, S. E. S., Fornaro,
701 A., Ynoue, R. Y., Artaxo, P., and Andrade, M. F.: Physical-chemical
702 characterisation of the particulate matter inside two road tunnels in the Sao
703 Paulo Metropolitan Area, *Atmos. Chem. Phys.*, 13, 12199-12213, 2013.

704 Brown, S. G., Lee, T., Roberts, P. T., and Collett, J. L. Jr.: Variations in the OM/OC ratio
705 of urban organic aerosol next to a major roadway, *J. Air & Waste Manag. Assoc.*,
706 63(12), 1422-1433, 2013.

707 Carvalho, V. S. B., Freitas, E. D., Martins, L. D., Martins, J. A., Mazzoli, C. R., and
 708 Andrade, M. F.: Air quality status and trends over the Metropolitan Area of
 709 Sao Paulo, Brazil as a result of emission control policies, *Environmental*
 710 *Science & Policy*, 47, 68-79, 2015.

711 Castanho, A. D. A. and Artaxo, P.: Sao Paulo aerosol source apportionment for
 712 wintertime and summertime, *Atmos. Environ.*, 35, 4889-4902, 2001.

713 Costa, R., Sodre, J. R.: Hidrous etanol vs. Gasoline-ethanol blend: engine performance
 714 and emissions, *Fuel*, 89, 287-293, 2010.

715 CETESB - Companhia de Tecnologia de Saneamento Ambiental. Relatorio Anual
 716 de Qualidade do Ar no Estado de Sao Paulo 2012, Sao Paulo, 2013.

717 CETESB - Companhia de Tecnologia de Saneamento Ambiental. Emissões
 718 veiculares no Estado de São Paulo 2011, Sao Paulo, 2012.

719 CETESB - Companhia de Tecnologia de Saneamento Ambiental. Relatorio Anual
 720 de Qualidade do Ar no Estado de Sao Paulo 2009, Sao Paulo, 2010.

721 Chang, J. S., Binkowski, F. S., Seaman, N. L., McHenry, J. N., Samson, P. J.,
 722 Stockwell, W. R., Walcek, C. J., Madronich, S., Middleton, P. B., Pleim, J. E.,
 723 and Lansford, H. H.: The regional acid deposition model and engineering
 724 model, *State-of-Science/Technology, Report 4*, National Acid Precipitation
 725 Assessment Program, Washington, DC, 1989.

726 Draxler, R. R. and Hess, G. D.: An overview of the HYSPLIT 4 modelling system of
 727 trajectories, dispersion, and deposition, *Aust. Meteor. Mag.*, 47, 295-308, 1998.

728 Emmons, L. K., Walters, S., Hess, P. G., Lamarque, F., Pfister, G. G., Fillmore, D.,
 729 Granier, C., Guenther, A., Kinnison, D., Laepple, T., Orlando, J., Tie, X.,
 730 Tyndall, G., Wiedinmyer, C., Baughcum, S. L., and Kloster, S.: Description

731 and evaluation of the Model for Ozone and Related chemical Tracers, version
732 4 (MOZART-4), Geosci. Model Dev., 3, 43-67, 2010.

733 Ginoux, P., Chin, M., Tegen, I., Prospero, J. M., Holben, B., Dubovik, O., and Lin,
734 S.-J.: Sources and distributions of dust aerosols simulated with the GOCART
735 model, Journal of Geophysical Research, 106, 20,255-20,273, 2001.

736 Gong, S. L.: A parameterization of sea-salt aerosol source function for sub- and
737 super-micron particles, Global Biogeochemical Cycles, 17, 1097,
738 doi:10.1029/2003GB002079, 2003.

739 Gorin, C. A., Collett, J. L. Jr., and Herckes, P.: Wood smoke contribution to winter
740 aerosol in Fresno, CA, J. Air & Waste Manag. Assoc., 56(11), 1584-1590,
741 2006.

742 GrEC – Grupo de Estudos Climáticos. Relatório climatológico mensal, previsão
743 climática para o Brasil: Set-Out-Nov/2012, Sao Paulo, 2012a. Available at:
744 www.grec.iag.usp.br/link_grec_old/relatorios_climatologicos/2012/agosto/

745 GrEC – Grupo de Estudos Climáticos. Relatório climatológico mensal, monitoramento
746 climático para o Brasil: Set/2012, Sao Paulo, 2012b. Available at:
747 www.grec.iag.usp.br/link_grec_old/relatorios_climatologicos/2012/setembro/

748 Grell, G. A., Peckham, S. E., Schmitz, R., McKeen, S. A., Wilczak, J., and Eder, B.:
749 Fully coupled “online” chemistry within the WRF model, Atmos. Environ., 39,
750 6957-6975, 2005.

751 Guenther, A. B., Zimmerman, P. R., Harley, P. C., Monson, R. K., and Fall, R.:
752 Isoprene and monoterpene emission rate variability: model evaluations and
753 sensitivity analyses, Journal of Geophysical Research, 98D, 12609-12617,
754 1993.

755 Guenther, A., Zimmerman, P., and Wildermuth, M.: Natural volatile organic
 756 compound emission rate estimates for US woodland landscapes, *Atmos.*
 757 *Environ.*, 28, 1197-1210, 1994.

758 Fast, J. D., Gustafson, W. I., Easter, R. C., Zaveri, R. A., Barnard, J. C., Chapman,
 759 E. G., Grell, G. A., and Peckham, S. E.: Evolution of ozone, particulates, and
 760 aerosol direct radiative forcing in the vicinity of Houston using a fully
 761 coupled meteorology-chemistry-aerosol module, *Journal of Geophysical*
 762 *Research*, 111, D21305, doi:10.1029/2005JD006721, 2006.

763 Forkel, R., Werhahn, J., Hansen, A. B., McKeen, S., Peckham, S., Grell, G., and
 764 Suppan, P.: Effect of aerosol-radiation feedback on regional air quality - A
 765 case study with WRF/Chem, *Atmospheric Environment*, 53, 202-211, 2012.

766 Heal, M. R., Kumar, P., and Harrison, R. M.: Particles, air quality, policy and health,
 767 *Chem. Soc. Rev.*, 41, 6606-6630, 2012.

768 Jenkin, M. E. and Clemitshaw, K. C.: Ozone and other secondary photochemical
 769 pollutants: chemical processes governing their formation in the planetary
 770 boundary layer, *Atmos. Environ.*, 34, 2499-2527, 2000.

771 Kroll, J. H. and Seinfeld, J. H.: Chemistry of secondary organic aerosol: Formation and
 772 evolution of low-volatility organics in the atmosphere, *Atmos. Environ.*, 42,
 773 3593-3624, 2008.

774 Kulmala, M., Laaksonen, A., and Pirjola, L.: Parameterization for sulphuric
 775 acid/water nucleation rates, *Journal of Geophysical Research*, 103,
 776 8301-8307, 1998.

777 Kumar, P., Morawska, L., Birmili, W., Paasonen, P., Hu, M., Kulmala, M., Harrison,
 778 R.M., Norford, L., and Britter, R.: Ultrafine particles in cities, *Environment*
 779 *International*, 66, 1-10, 2014.

780 Kumar, P., Robins, A., Vardoulakis, S., and Britter, R.: A review of the characteristics
 781 of nanoparticles in the urban atmosphere and the prospects for developing
 782 regulatory control, *Atmos. Environ.*, 44, 5035-5052, 2010.

783 Kumar, P., Ketzel, M., Vardoulakis, S., Pirjola, L., Britter, R.: Dynamics and dispersion
 784 modelling of nanoparticles from road traffic in the urban atmospheric
 785 environment - a review, *J. Aerosol Sci.*, 42, 580-603, 2011.

786 Li, G., Bei, N., Tie, X., and Molina, L. T.: Aerosol effects on the photochemistry in
 787 Mexico City during MCMA-2006/MILAGRO campaign, *Atmos. Chem. Phys.*,
 788 11, 5169-5182, 2011a.

789 Li, G., Zavala, M., Lei, W., Tsimpidi, A. P., Karydis, V. A., Pandis, S. N., Canagaratna,
 790 M. R., and Molina, L. T.: Simulations of organic aerosol concentrations in
 791 Mexico City using the WRF-Chem model during the
 792 MCMA-2006/MILAGRO campaign, *Atmos. Chem. Phys.*, 11, 3789-3809,
 793 2011b.

794 Li, G., Zhang, R., and Fan, J.: Impacts of black carbon aerosol on photolysis and
 795 ozone, *Journal of Geophysical Research*, 110, D23206,
 796 doi:10.1029/2005JD005898, 2005.

797 Marple, V. A., Rubow, K. L., Ananth, G. P., and Fissan, H. J.: Micro-Orifice uniform
 798 deposit impactor, *Journal of Aerosol Science*, 17, 489-494, 1986.

799 Martins, L. D., Vasconcellos, P.C., Carvalho, L. F., Andrade, M.F.: Estimated impact of
 800 biogenic hydrocarbon emissions on photochemical oxidant formation in São
 801 Paulo during two periods of the winters of 1999-2000, *Revista Brasileira de*
 802 *Meteorologia*, 21, 190-200, 2006.

803 McMurry, P., Shepherd, M., and Vickery, J.: Particulate Matter Science for Policy
804 Makers: A NARSTO Assessment, Cambridge University Press, Cambridge,
805 England, 2004.

806 Middleton, P., Stockwell, W. R., and Carter, W. P. L.: Aggregation and analysis of
807 volatile organic compound emissions for regional modelling, *Atmos.*
808 *Environ.*, 24A, 1107-1133, 1990.

809 Miranda, R. M. and Andrade, M. F.: Physicochemical characteristics of atmospheric
810 aerosols during winter in the Sao Paulo Metropolitan Area in Brazil, *Atmos.*
811 *Environ.*, 39, 6188-6193, 2005.

812 Monahan, E. C., Spiel, D. E., Davidson, K. L.: A model of marine aerosol generation
813 via whitecaps and wave disruption. In: Monahan, E. C., MacNiocaill, G. D.
814 (Eds.), *Oceanic Whitecaps*. Reidel Publishing Company, Norwell, Mass,
815 167-174, 1986.

816 Muñoz, A. G., López, P., Velásquez, R., Monterrey, L., León, G., Ruiz, F., Recalde,
817 C., Cadena, J., Mejía, R., Paredes, M., Bazo, J., Reyes, C., Carrasco, G.,
818 Castellón, Y., Villarroel, C., Quintana, J., and Urdaneta, A.: An
819 Environmental Watch System for the Andean Countries: El Observatorio
820 Andino, *Bull. Amer. Meteor. Soc.*, 91, 1645-1652, 2010.

821 Muñoz, A. G., Ruiz-Carrascal, D., Ramírez, P., León, G., Quintana, J., Bonilla, A.,
822 Torres, W., Pastén, M., and Sánchez, O.: Risk Management at the Latin
823 American Observatory, in: *Risk Management – Current Issues and*
824 *Challenges*, InTech Publications, doi:10.5772/50788, 533-556, 2012.

825 Nogueira, T., Dominutti, P. A., De Carvalho, L. R. F., Fornaro, A., and Andrade, M.
826 F.: Formaldehyde and acetaldehyde measurements in urban atmosphere

827 impacted by the use of ethanol biofuel: Metropolitan Area of Sao Paulo,
 828 2012-2013, *Fuel*, 134, 505-513, 2014.

829 Odum, J. R., Hoffmann, T., Bowman, F., Collins, D., Flagan, R. C., and Seinfeld, J.
 830 H.: Gas/particle partitioning and secondary organic aerosol yields,
 831 *Environmental Science Technology*, 30, 2580-2585, 1996.

832 Pankow, J. F.: An absorption model of the gas aerosol partitioning involved in the
 833 formation of secondary organic aerosol, *Atmos. Environ.*, 28, 185-188,
 834 1994a.

835 Pankow, J. F.: An absorption model of the gas aerosol partitioning involved in the
 836 formation of secondary organic aerosol, *Atmos. Environ.*, 28, 189-93,
 837 1994b.

838 Pérez-Martínez, P. J., Miranda, R. M., Nogueira, T., Guardani, M. L., Fornaro, A.,
 839 Ynoue, R., and Andrade, M. F.: Emission factors of air pollutants from
 840 vehicles measured inside road tunnels in Sao Paulo: case study comparison,
 841 *Int. J. Environ. Sci. Technol.*, 11, 2155-2168, 2014.

842 Real, E. and Sartelet, K.: Modelling of photolysis rates over Europe: impact on
 843 chemical gaseous species and aerosols, *Atmos. Chem. Phys.*, 11, 1711-1727,
 844 2011.

845 Salvo, A. and Geiger, F. M.: Reduction in local ozone levels in urban Sao Paulo due to a
 846 shift from ethanol to gasoline use, *Nature Geoscience*, 7, 450-458,
 847 doi:10.1038/ngeo2144, 2014.

848 Saxena, P., Hudischewskyj, A. B., Seigneur, C., and Seinfeld, J. H.: A comparative
 849 study of equilibrium approaches to the chemical characterization of
 850 secondary aerosols, *Atmos. Environ.*, 20, 1471-1483, 1986.

851 Schell, B., Ackerman, I. J., Hass, H., Binkowski, F. S., and Ebel, A.: Modelling the
 852 formation of secondary organic aerosol within a comprehensive air quality
 853 model system, *Journal of Geophysical Research*, 106, 28275-28293, 2001.

854 Seinfeld, J. H. and Pandis, S. N.: *Atmospheric Chemistry and Physics: from air*
 855 *pollution to climate change*, Second Edition, Jhon Wiley, New Jersey,
 856 2006.

857 Shrivastava, M., Berg, L. K., Fast, J. F., Easter, R. C., Laskin, A., Chapman, E. G.,
 858 Gustafson Jr, W. I., Liu, Y., and Berkowitz, C. M.: Modelling aerosols and
 859 their interactions with shallow cumuli during the 2007 CHAPS field study,
 860 *Journal of Geophysical Research: Atmospheres*, 118, 1343-1360, 2013.

861 Taylor, K. E.: Summarizing multiple aspects of model performance in a single diagram,
 862 *Journal of Geophysical Research*, 106(D7), 7183-7192,
 863 doi:10.1029/2000JD900719, 2001.

864 Tuccella, P., Curci, G., Visconti, G., Bessagnet, B., Menut, L., and Park, R. J.:
 865 Modelling of gas and aerosol with WRF-Chem over Europe: Evaluation and
 866 sensitivity study, *Journal of Geophysical Research*, 117, D03303,
 867 doi:10.1029/2011JD016302, 2012.

868 Vasconcellos, P. C., Souza, D. Z., Sanchez-Ccoyllo, O. R., Bustillos, J. O. V., Lee,
 869 H., Santos, F. C., Nascimento, K. H., Araujo, M. P., Saarnio, K., Teinila, K.,
 870 and Hillamo, R.: Determination of anthropogenic and biogenic
 871 compounds on atmospheric aerosol collected in urban, biomass burning
 872 and forest areas in Sao Paulo, Brazil, *Science of the Total Environment*, 408,
 873 5836-5844, 2010.

874 Vieira-Filho, M. S., Pedrotti, J. J., and Fornaro, A.: Contribution of long and mid-range
875 transport on the sodium and potassium concentrations in rainwater samples, Sao
876 Paulo megacity, Brazil, *Atmos. Environ.*, 79, 299-307, 2013.

877 Wedding, J. B., Weigand, M., John, W. and Wall, S.: Sampling effectiveness of the inlet
878 to the dichotomous sampler, *Environ. Sci. Technol.*, 14(11), 1367-1370, 1980.

879 Ynoue, R. Y. and Andrade, M. F.: Size-resolved mass balance of aerosol particles over
880 the Sao Paulo Metropolitan Area of Brazil, *Aerosol Science and Technology*,
881 1, 52-62, 2004.

882 Table 1. Description of aerosol sampling campaigns performed at IAG-USP.

Parameter	Sampling frequency	Period of sampling	Sampling device
Aerosol mass size distribution	24 hours	July-September	MOUDI impactor
PM _{2.5} and PM ₁₀ concentration	12 hours	July-September	PARTISOL sampler
OC and EC concentration	12 hours	August-September	Sunset OC-EC analyser

883

884

885 Table 2. Description of measurement sites.

Initials	Name	Latitude	Longitude	Measured species
NSO	Nossa S. do O	-23.4796	-46.6916	PM ₁₀ , O ₃
SAN	Santana	-23.5055	-46.6285	PM ₁₀
PDP	Parque D. Pedro	-23.5448	-46.6276	PM ₁₀ , O ₃
MOO	Mooca	-23.5497	-46.5984	PM ₁₀ , O ₃
CCE	Cerqueira Cesar	-23.5531	-46.6723	PM ₁₀
IAG-USP	IAG-USP	-23.5590	-46.7330	PM ₁₀ , PM _{2.5} , OC, EC Aerosol mass size distrib. ^a
IPEN-USP	IPEN-USP	-23.5662	-46.7374	PM _{2.5} , O ₃ , NO _x , CO
IBI	Ibirapuera	-23.5914	-46.6602	PM ₁₀ , O ₃ , NO _x , CO
CON	Congonhas	-23.6159	-46.6630	PM ₁₀ , PM _{2.5}
AF-IAG	AF-IAG	-23.6500	-46.6167	T, RH, WS, WD ^b
SAM	Santo Amaro	-23.6545	-46.7095	PM ₁₀
INT	Interlagos	-23.6805	-46.6750	PM ₁₀ , O ₃ , T, RH, WS, WD

886 ^aincludes SO₄²⁻, NO₃⁻, NH₄⁺, Na⁺, Cl⁻ and PM₁₀.

887 ^bT, RH, WS, and WD denote temperature, relative humidity, wind speed and wind
888 direction, respectively.

889

890 Table 3. Selected WRF-Chem configuration options.

Atmospheric Process	WRF-Chem option
Longwave radiation	RRTM
Shortwave radiation	Goddard
Surface layer	Monin - Obukhov
Land surface	Noah
Boundary layer	YSU
Cumulus clouds ^a	Grell 3D
Cloud microphysics	Lin
Gas-phase chemistry	RADM2
Aerosol chemistry	MADE/SORGAM
Photolysis	Fast-J

891 ^aOuter domains only

892

893 Table 4. Description of WRF-Chem simulations.

Label	Description
Case_0 (Baseline simulation)	Emission of gases
	Emission of aerosols
	Aerosol - radiation feedback turned on
Case_1	Emission of gases
	No emission of aerosols
	Aerosol - radiation feedback turned on
Case_2	Emission of gases
	Emission of aerosols
	Aerosol - radiation feedback turned off

894

895

Table 5. Performance statistics for WRF-Chem predictions at all sites^a

Index	PM _{2.5}	PM ₁₀	O ₃	NO _x	CO	T	RH	U ^b	V ^c
R	0.73	0.72	0.63	0.42	0.54	0.71	0.62	0.48	0.44
B	-8.84	-14.1	-0.85	-8.75	-0.27	0.65	-5.74	-0.96	0.75
RMSE _{UB}	6.83	10.59	27.45	30.35	0.57	3.21	20.06	1.04	1.02

^aValues are averaged from all the individual indexes found at the measurement sites.

Individual indexes are calculated from both hourly observed and predicted values.

^bZonal wind component

^cMeridional wind component

Figure 1. Downtown area of the 3-km modelling domain (d03) showing the locations of measurement sites and WRF topography in the vicinity of SPMA. Red dots represent sites with information on O₃ and aerosol. Yellow dots represent only sites with information on PM. Blue dot represents the location of the IAG-USP's climatological station.

Figure 2. Emission rates for Aromatic VOCs at 19 UTC in the 3-km modelling domain.

Figure 3. Hourly accumulated precipitation and relative humidity observed at the IAG-USP's climatological station during the study period.

Figure 4. HYSPLIT three-day backward trajectories and locations of fires in Sao Paulo State and part of central-west region of Brazil. Pink markers represent the observed fire locations during the study period considering different satellite products (GOES, AQUA, TERRA, NOAA). The backward trajectories starting at IAG-USP were calculated for the days 9 and 31 August and 5 September 2012 at three different altitudes: 500 m (red lines), 1000 m (blue lines), and 2000 m (green lines).

Figure 5. Daily (top), diurnal (bottom), and nocturnal (middle) mean concentrations for EC, OC, PM₁₀, PM_{2.5-10}, PM_{2.5} (left panels), and Na, Fe₂SO₃, SiO₂, K₂O, and S (right panels). The PM_{2.5-10} aerosol variable is defined as particulate matter with aerodynamic between 2.5 and 10 µm. The grey line indicates the WHO air quality standard for PM_{2.5} (25 µg/m³).

Figure 6. The predicted average of wind vectors at 10 m and temperature at 2 m from the baseline simulation (Case_0) for the whole study period in the 3-km modelling domain. Blue dots represent the location of the measurement sites,

whereas cyan numbers represent the observed average temperature in those sites: 17.7 C in AF-IAG and 17.8 C in INT.

Figure 7. The observed and predicted daily variations of PM_{2.5} concentrations at 3 sites in SPMA for the 3-km modelling domain.

Figure 8. The observed and predicted daily variations of PM₁₀ concentrations at 10 sites in SPMA for the 3-km modelling domain.

Figure 9. The observed and predicted hourly variations of O₃ concentrations at six sites in SPMA for the 3-km modelling domain.

Figure 10. Taylor diagram showing the individual correlation coefficients, bias, and normalized standard deviations for the PM_{2.5}, PM₁₀, and O₃ concentrations.

Figure 11. The predicted average surface distribution of PM_{2.5} concentrations for the whole study period in the 3-km modelling domain. Red dots represent the location of the measurement sites with information on PM_{2.5}, whereas cyan numbers represent the observed average PM_{2.5} concentration in those sites: 23.4 µg m⁻³ in IPEN-USP, 21.3 µg m⁻³ in IAG-USP, and 22.2 µg m⁻³ in CON.

Figure 12. The predicted average surface distribution of PM₁₀ concentrations for the whole study period in the 3-km modelling domain. Red dots represent the location of the measurement sites with information on PM₁₀, whereas cyan numbers represent the observed average PM_{2.5} concentration in those sites: 49.5 µg m⁻³ in IAG-USP and 38.7 µg m⁻³ in CON.

Figure 13. The predicted average surface distribution of the PM_{2.5}/PM₁₀ ratio for the whole study period in the 3-km modelling domain. Red dots represent the location of the measurement sites with information on both PM_{2.5} and PM₁₀, whereas cyan numbers represent the observed average PM_{2.5}:PM₁₀ ratio in those sites: 0.43 in IAG-USP and 0.57 in CON.

Figure 14. The observed and predicted daily variations of OC and EC concentrations at IAG-USP.

Figure 15. The observed and predicted average aerosol mass size distribution for SO_4 , NO_3 , NH_4 , Na, Cl, and other PM_{10} constituents at IAG-USP. The observed aerosol distributions were collected in ten size classes using a rotated impactor (MOUDI) and joined adequately according to the three modes used by the MADE aerosol module: Aitken ($<0.1 \mu\text{m}$), accumulation ($0.1\text{--}1 \mu\text{m}$) and coarse ($>1 \mu\text{m}$). The five inorganic ions carried in MADE are only calculated for the Aitken and accumulation modes. The WRF's PM_{10} aerosol variable does not include neither OC nor EC for this comparison.

Figure 16. The observed and predicted average contributions for the main identified constituents of $\text{PM}_{2.5}$ at IAG-USP.

Figure 17. The contribution of (a) gas emissions on the fine particles formation, (b) dust – sea salt emissions on the PM_{10} concentration, and (c) aerosol direct effect on the ground level O_3 concentrations at 16:00 LT.